

Phenylhydrazone Derivatives as Corrosion Inhibitors for α -Brass in Hydrochloric Acid Solutions

M. Abdallah¹, M. Al-Agez¹ and A.S. Fouda²

¹ Chem. Dept. Faculty of Science , Benha University, Benha. Egypt

² Chem. Dept. Faculty of Science , Mansoura University ,Mansoura . Egypt

E-mail: metwally552@hotmail.com

Received: 1 November 2008 / Accepted: 29 January 2009 / Published: 1 March 2009

The inhibition effect of some phenylhydrazone derivatives, namely, [ethyl(2Z)-cyano[(4E)-5-oxo-3-phenyl-4-(phenylhydrazono)-1,3-thiazolidin-2-ylidene] acetate (A), ethyl(2Z)-cyano[(4E)-5-oxo-3-phenyl-4-(p-methylphenylhydrazono)-1,3-thiazolidin-2-ylidene] acetate (B), ethyl(2Z)-cyano[(4E)-5-oxo-3-phenyl-4-(o-methoxyphenylhydrazono)-1,3-thiazolidin-2-ylidene] acetate (C) and ethyl(2Z)-cyano[(4E)-5-oxo-3-thiazolidin-2-ylidene] acetate (D) on the corrosion of 70Cu-30Zn brass in 2M HCl solution has been investigated using weight loss and galvanostatic polarization techniques. The percentage inhibition efficiency was found to increase with increasing concentration of inhibitor and with decreasing temperature. The addition of KI to phenylhydrazone derivatives enhanced the inhibition efficiency due to synergistic effect. The adsorption of these inhibitors on the brass surface obeys Temkin isotherm. Some activated thermodynamic parameters were calculated. The addition of these compounds to the potentiodynamic anodic polarization curves of α -brass electrode in chloride solutions shift the pitting potential to more positive values, indicating an increased resistance to pitting attack.

Keywords: α -brass , phenylhydrazone derivatives, corrosion inhibitors

1. INTRODUCTION

Copper and its alloys are widely used in industry because of their excellent electrical and thermal conductivity and are often used in heating and cooling system [1–3]. Brass has been widely used as tubing material for condensers and heat exchangers in various cooling water systems [4–9]. Brass is susceptible to a corrosion process known as dezincification and this tendency increases with increasing zinc content of the brass [10,11]. During the past decade, many techniques have been used to minimize the dezincification and corrosion of brasses. One of the techniques for minimizing corrosion is the use of inhibitors. The effectiveness of the inhibitor varies with its concentration, the

corrosive medium and the surface properties of the alloy. Many inhibitors have been used to minimize the corrosion of brass in different media. Particularly, heterocyclic organic compounds containing nitrogen, sulphur and/or oxygen atoms are often used to protect metals from corrosion, e.g. amino-pyrazole [12-14], amino-thiazole and triazole thiols [15,16], found many applications in corrosion inhibition of copper alloys. Benzimidazole and its derivatives have been shown to inhibit dissolution of brass in H_2SO_4 [17]. The effect of tetrazole compounds on the corrosion of brass (70Cu–30Zn) in sulphuric acid solution has been investigated [18]. The effectiveness of heterocyclic molecules as corrosion inhibitors is based on their chelating action and the formation of an insoluble physical diffusion barrier on the electrode surface, preventing metal reaction and dissolution. The studies show that copper surface is normally coated with a layer of cuprous oxide CuO [19], and these inhibitors form protective barriers of inert, insoluble and long-lasting polymeric $Cu(I)$ complex coatings on the CuO substrate. These polymeric complex coatings are thermally stable, thereby inhibiting the corrosion process [20–28]. $Cu(I)$ is formally bonded to N or S or O atoms of the inhibitor molecules. As predicted, films formed by different inhibitors have shown differences in their corrosion protection. Formation of $Cu(II)$ complexes also can occur, but they do not appear to be protective [22]

The aim of the present work is to study the effect of some phenylhydrazone derivatives as corrosion inhibitors for dissolution of α -brass in 2M HCl solutions using weight loss and galvanostatic polarization measurements. The effect of temperature on the dissolution of α -brass in free and inhibited acid solution was also, investigated. Moreover, the ability of these compounds to provide a protection against pitting corrosion was studied using potentiodynamic anodic polarization technique.

2. EXPERIMENTAL PART

The experiments were performed with α -brass having the chemical compositions Cu 70 % and Zn 30 % Weight loss measurements were performed using coupons of the dimensions 2.0 x 2.0 x 0.2 cm. For galvanostatic and potentiodynamic anodic polarization measurements, a cylindrical rod embedded in araldite with exposed surface of 0.3 cm^2 was used. The electrode was polished with different grades of emery paper, degreased with acetone and rinsed by distilled water. For galvanostatic experiments, the electrode was put under open circuit potential until stable potential was attained (about 30 min) and for potentiodynamic anodic polarization experiments, the electrode was held at hydrogen evolution potential for 10 min in order to get rid of any pre-immersion oxide film. Weight loss measurements were carried out as described elsewhere [29]. The percentage inhibition efficiency (% IE) and a parameter (θ) which represents the part of the metal surface covered by the inhibitor molecules were calculated using the following equations:

$$\% IE = \frac{W_{free} - W_{inh}}{W_{free}} \times 100 \quad (1)$$

$$\theta = \frac{W_{free} - W_{inh}}{W_{free}} \quad (2)$$

where W and W_i are the weight-loss per unit area in absence and presence of the additive, respectively.

Galvanostatic polarization studies were carried out using EG&G model 173 potentiostat/galvanostat. Three compartment cell with a saturated calomel reference electrode and a platinum foil auxiliary electrode was used. The percentage inhibition efficiency (% IE) was calculated from corrosion current density values using the equation

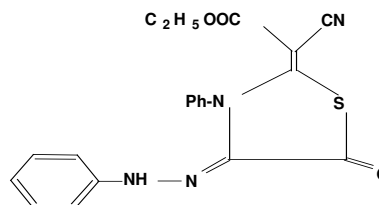
$$\% \text{ IE} = (1 - i_{\text{inh.}}/i_{\text{free}}) \times 100 \quad (3)$$

where i_{free} and $i_{\text{inh.}}$ are the corrosion currents in absence and in presence of the inhibitor.

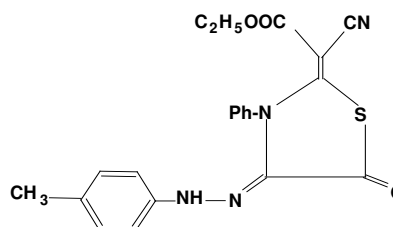
Potentiodynamic anodic polarization technique was performed at a scanning rate of 1 mV/s using a Wenking potentiostat type POS 73 and the current density-potential curve were recorded on X-Y recorder type PL.3. The potentials were measured relative to a saturated calomel electrode (SCE) and the electrolytic cell is described elsewhere [30]

The inhibitors used in this study were selected from phenylhydrazone derivatives and their chemical structure are

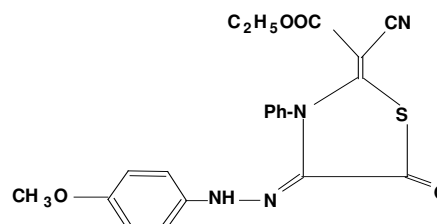
Compound (A): Ethyl(2Z)-cyano[(4E)-5-oxo-3-phenyl-4(phenylhydrazono)-1,3 thiazolidin-2-ylidene] acetate.



Compound (B): Ethyl(2Z)-cyano[(4E)-5-oxo-3-phenyl-4-(p-methylphenylhydrazono)-1,3-thiazolidin-2-ylidene] acetate.



Compound (C) :Ethyl(2Z)-cyano[(4E)-5-oxo-3-phenyl-4-(p-methoxyphenylhydrazono)-1,3-thiazolidin-2-ylidene] acetate.



Compound (D): Ethyl(2Z)-cyano[(4E)-5-oxo-3-phenyl-4-(p-nitrophenylhydrazone)-1,3-thiazolidin-2-ylidene] acetate.

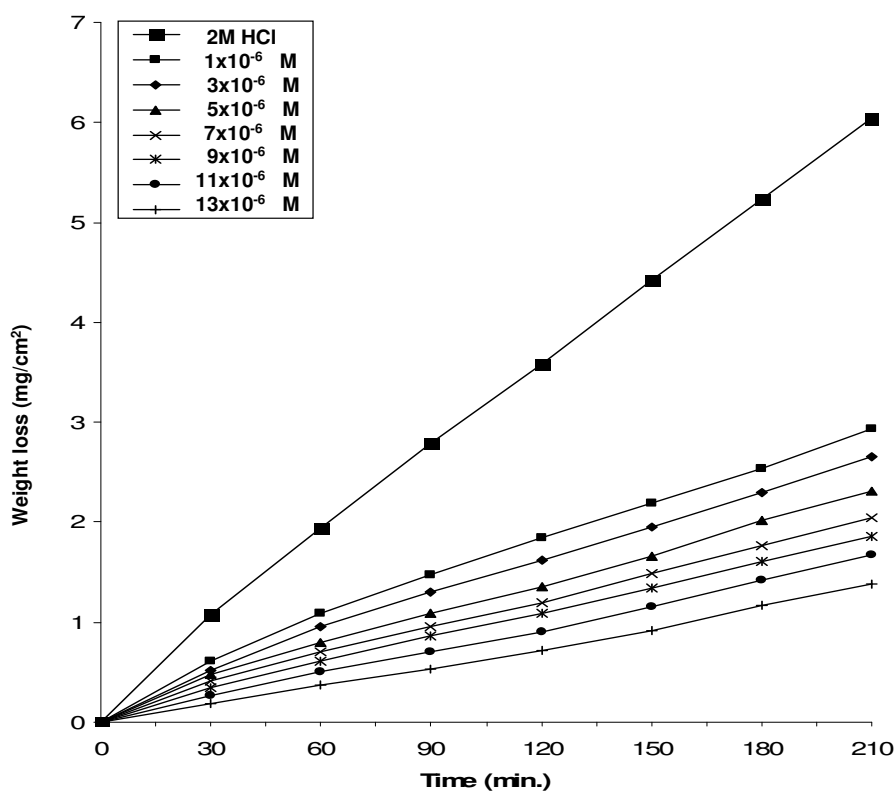
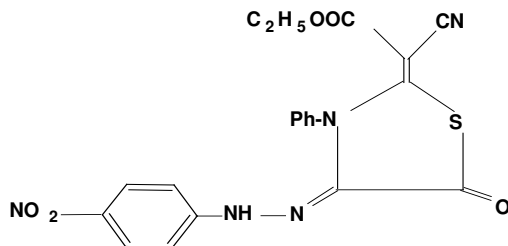


Figure 1. Weight loss-time curves of α -brass in 2M HCl in presence and absence of different concentrations of inhibitor (c) at 303K

3. RESULTS AND DISCUSSION

3.1. Weight loss measurements

Fig.1 shows the weight loss- time curves for α -brass coupons in 2 M HCl solution devoid of and containing different concentrations of compound (C) as an example. Similar curves were also obtained for other three compounds (not shown). Inspection of this figure reveals that, the curves are

characterized by gradual rise in weight loss with time. The curves indicate that, the weight loss of brass depends on the concentration of additives. The calculated values of inhibition efficiencies obtained from weight loss are listed in Table (1). It is obvious that the IE increases with increasing the inhibitor concentration, whereas decreases in the following order:

compound C > compound B > compound A > compound D.

This behavior will be discussed later.

3.2. Synergistic effect of KI

The effect of KI on the inhibitive performance of phenylhydrazone derivatives has been studied using weight loss technique. The values of IE for specific concentration of KI (1×10^{-3} M) in the presence of various concentrations of inhibitors are given in Table (2). The synergistic inhibition effect was evaluated using a parameter, S_θ , obtained from the surface coverage θ of the anion, cation and both. Aramaki and Hackerman [31].

calculated the synergistic parameter, S_θ , using the following equation:

$$S_\theta = 1 - \theta_1 + 2 / 1 - \theta_{1+2} \quad (4)$$

where: $\theta_{1+2} = (\theta_1 + \theta_2) - (\theta_1\theta_2)$; θ_1 is the surface coverage of cation (protonated inhibitor); θ_2 is the surface coverage of anion (I); θ_{1+2} is the measured surface coverage by both the anion (I) and the cation (protonated inhibitor). The calculated values of S_θ are given in Table (3). Inspection of Table (1), the values of S_θ are nearly equal to unity which suggests that the enhanced inhibition efficiencies caused by the addition of iodide ions to phenylhydrazone compounds is due mainly to the synergistic effect. In case of presence of this mixture, the K^+ ion is chelated by hydrazone nucleus via lone pair of electrons on one nitrogen atom, and the iodide ion is more free i.e. more adsorbed on the steel surface. Hence the values of inhibition efficiency increase than the value of IE of each additive separately.

Table 1. Inhibition efficiency at different concentrations of inhibitors as determined by weight loss method at 303K and 210 min immersion

[Inhibitor] M	% Inhibition			
	A	B	C	D
1×10^{-6}	47.0	54.4	61	23.0
3×10^{-6}	51.3	58.6	69.2	31.0
5×10^{-6}	55.7	62.8	73.5	42.4
7×10^{-6}	59.8	67.4	77.8	49.7
9×10^{-6}	65.0	71.7	81.5	60.0
11×10^{-6}	68.8	75.3	84.1	64.0
13×10^{-6}	71.9	79.1	86.4	67.8

Table 2. Inhibition efficiency at different concentrations of inhibitors in presence of 1×10^{-3} M of KI as determined from weight loss method at 303K.

[Inhibitor] M	% Inhibition			
	A	B	C	D
1×10^{-6}	74.6	77.7	80.5	63.5
3×10^{-6}	77.0	80.2	84.8	68.0
5×10^{-6}	79.4	82.5	87.2	73.7
7×10^{-6}	81.6	84.9	89.5	77.4
9×10^{-6}	84.2	87.0	91.3	82.3
11×10^{-6}	86.1	88.8	92.6	84.3
13×10^{-6}	87.7	90.7	93.8	86.1

Table 3. Synergistic parameters (S_{θ}) for different concentrations of all used inhibitors in 2M HCl in presence of 1×10^{-3} M of KI.

[Inhibitor] M	(S_{θ})			
	A	B	C	D
1×10^{-6}	0.9411	0.9264	0.902	0.9514
3×10^{-6}	0.9549	0.943	0.9169	0.9711
5×10^{-6}	0.9677	0.9561	0.9302	0.986
7×10^{-6}	0.9829	0.9707	0.9483	1.0018
9×10^{-6}	0.9962	0.9859	0.959	1.0192
11×10^{-6}	1.0123	1.0036	0.973	1.0341
13×10^{-6}	1.0303	1.0146	0.9893	1.0448

3.3. Effect of temperature

The effect of temperature on the corrosion rate of α -brass in 2M HCl and in presence of different inhibitors concentrations was studied in the temperature range of 303–328K using weight loss measurements. Similar curves to Fig. 1 were obtained (not shown). As the temperature increases, the rate of corrosion increases and hence the inhibition efficiency of the additives decreases. This is due to the desorption is aided by increasing the temperature. This behavior proves that the adsorption of inhibitors on α -brass surface occurs through physical adsorption. The apparent activation energy E_a^* , the enthalpy of activation ΔH and entropy of activation ΔS^* for the corrosion of α -brass in 2M HCl solutions in absence and presence of different concentrations of phenylhydrazone derivatives were calculated from Arrhenius-type equation [32].

$$k = A \exp(E_a^*/RT) \quad (5)$$

and transition state equation

$$k = (RT/Nh) \exp(\Delta S^*/R) \exp(-\Delta H^*/RT) \quad (6)$$

where k is the rate of metal dissolution, A is the frequency factor, N is Avogadro's number and R is the universal gas constant.

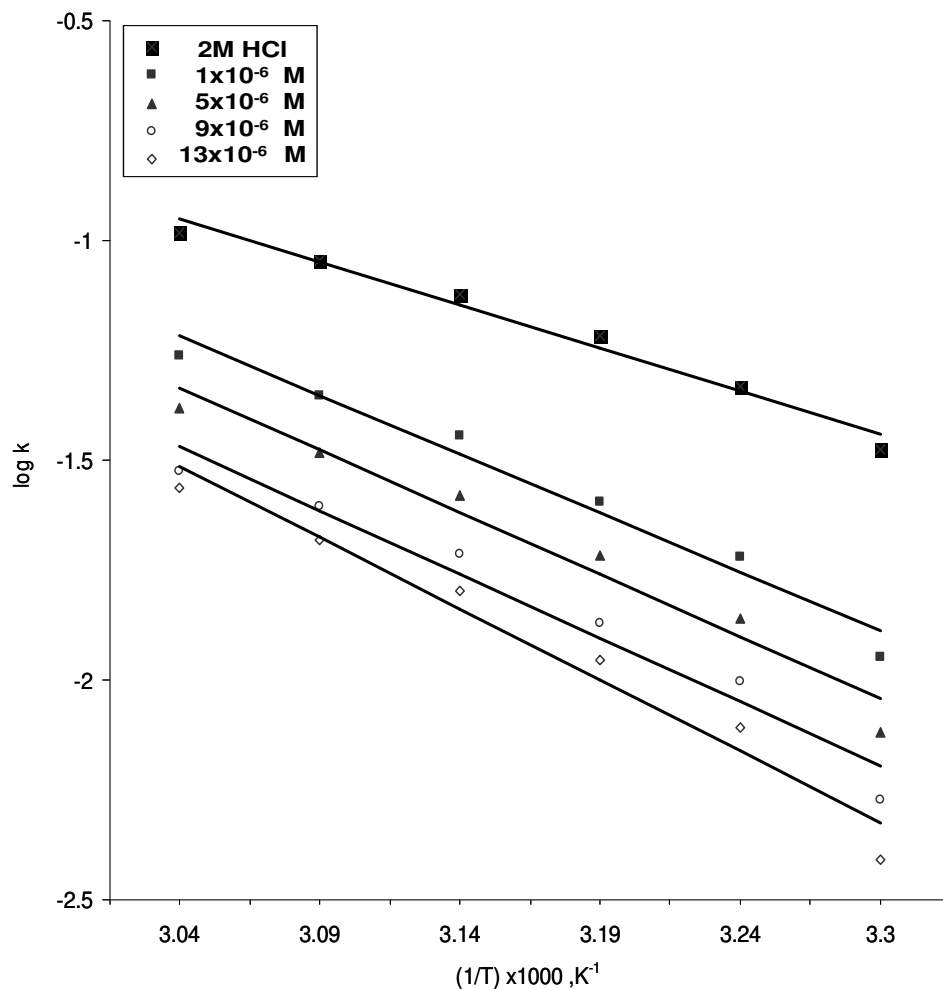


Figure 2. Log (k) vs. ($1/T$) curves for α -brass dissolution in 2M HCl in the presence and absence of different concentration of inhibitor (C)

Fig. 2 represents plot of $\log k$ against $1/T$ for α -brass in 2 M HCl solution in absence and presence of different concentrations of compound C as an example. Similar curves were obtained for other compounds (not shown). Straight lines were obtained with slope equal to $-E_a^*/2.303R$. The values of E_a^* for the corrosion reaction in the absence and presence of different compounds was calculated and given in Table 4. Inspection of Table 4 demonstrates that, the presence of phenylhydrazone derivatives increases the values of E_a^* indicating the adsorption of the inhibitor molecule on the metal surface. The values of E_a^* increases with increasing the concentration of inhibitor. This mean that, the presence of derivatives induce an energy barrier for the corrosion reaction and this barrier increases with increasing the concentration of these compounds. On the other

hand, Fig. 3 represents the plots of $\log k/T$ against $1/T$ for α -brass in 2M HCl solution in absence and presence of different concentrations of compound C. Similar curves obtained for other compounds (not shown). This relation gave straight lines with slope equals to $\Delta H^*/2.303R$ and the intercept is $\log R/Nh + \Delta S^*/2.303R$. The obtained values of ΔH^* and ΔS^* are given in Table 4. The positive values of ΔH^* reflect that the process of dsorption of the inhibitors on the brass surface is endothermic process. The values of ΔS^* in the presence and absence of the inhibitors is large and negative. This implies that the activated complex is the rate determining step represents association rather than dissociation, This indicates that a decrease in disorder takes place going from reactants to the activated complex [33].

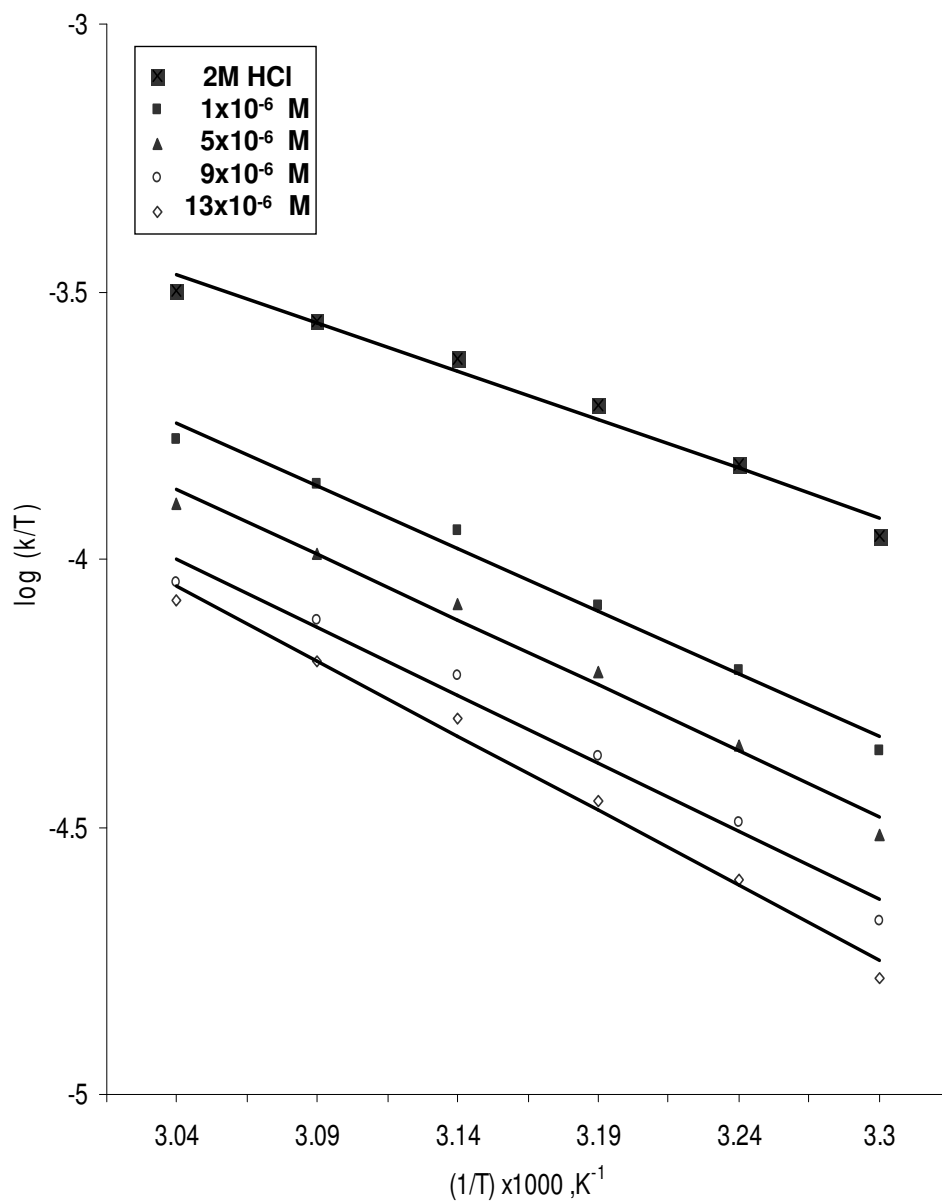


Figure 3. Log (k/T) vs. (1/T) curves for α -brass dissolution in 2M HCl in the presence and absence of different concentration of inhibitor (C)

Table 4. Activation parameters for the dissolution of α -brass in presence and absence of different concentrations of inhibitors in 2M HCl.

Activation parameters			Concentration M	Inhibitor
$-\Delta S_a^*$ J.mol ⁻¹ K ⁻¹	ΔH_a^* KJ.mol ⁻¹	E_a^* KJ.mol ⁻¹		
262.22	1.739	1.871	2.0	Free Acid
263.08	2.27	2.40	1x10⁻⁶	A
265.99	2.34	2.47	5x10⁻⁶	
267.56	2.40	2.53	9x10⁻⁶	
268.43	2.55	2.68	13x10⁻⁶	
265.78	2.34	2.47	1x10⁻⁶	B
266.95	2.41	2.55	5x10⁻⁶	
268.44	2.54	2.67	9x10⁻⁶	
270.14	2.67	2.80	13x10⁻⁶	
266.61	2.44	2.57	1x10⁻⁶	C
268.73	2.58	2.71	5x10⁻⁶	
271.2	2.65	2.79	9x10⁻⁶	
271.75	2.97	3.1	13x10⁻⁶	
262.35	2.18	2.31	1x10⁻⁶	D
264.18	2.27	2.40	5x10⁻⁶	
266.64	2.38	2.51	9x10⁻⁶	
267.81	2.47	2.60	13x10⁻⁶	

3.4. Adsorption isotherm

The values of the degree of surface coverage θ were evaluated at different concentrations of the inhibitors in 2M HCl solution. Attempts were made to fit θ values to various adsorption isotherm. The Temkin adsorption isotherm fits the experimental data. A plot of θ against $\log C$ for all concentrations of inhibitors Fig. 4 approximately a straight line relationship in all cases was obtained. This suggests that the adsorption of phenylhydrazones derivatives on the brass surface follow Temkin isotherm. These results confirm the assumption that, these compounds are adsorbed on the metal surface through the protonated (N,S,O) atoms or via the lone pair of electrons of (N,S,O) atoms. The extent of inhibition is directly related to the performance of adsorption layer which is a sensitive function of the molecular structure.

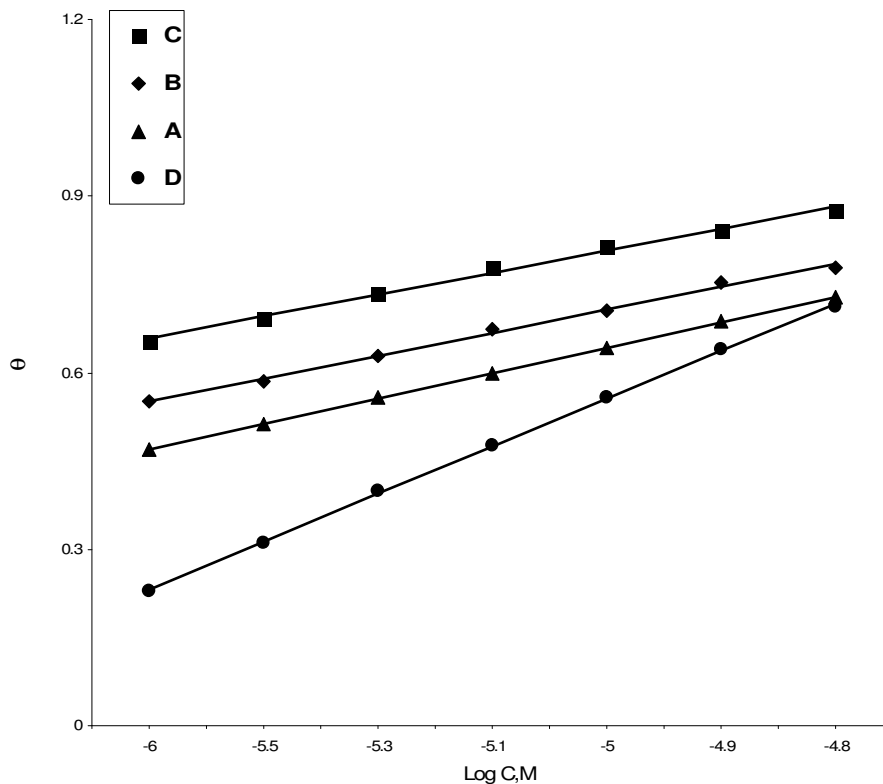


Figure 4. Curve fitting of corrosion data for α -brass in 2M HCl in presence of different concentrations of inhibitors to the Temkin's adsorption isotherm at 303K

3.5. Galvanostatic polarization studies

Fig. 5 shows the galvanosttic polarization curves for α -brass electrode in 2M HCl in the absence and presence of different concentrations of compound (C) at 30°C. Similar curves were obtained for other compounds (not shown).

The numerical values of the variation of the corrosion current density (I_{corr}) and corrosion potential (E_{corr}), Tafel slope (β_a & β_c), the degree of surface coverage (θ) and the inhibition efficiency (IE) with the concentrations of inhibitors are given in Table 5. The corrosion current density (I_{corr}) and corrosion potential (E_{corr}) were determined by the intersection of the extrapolating anodic and cathodic Tafel lines. Inspection of Table (5) reveals that :

- The values of E_{corr} is shifted nearly to more negative values and the values of I_{corr} decreases with increasing the concentration of the tested compounds which indicates that these compounds acts as an inhibitors, and the degree of inhibition depends on the concentration and type of inhibitors present.

- b) The anodic (β_a) and cathodic (β_c) Tafel slopes were changed on increasing the concentrations of the tested compounds. This means that these compounds are mixed type inhibitors.
- c) The orders of inhibition efficiency of all inhibitors at different concentration are given by polarization decreases in the following orders.

compound C > compound B > compound A > compound D

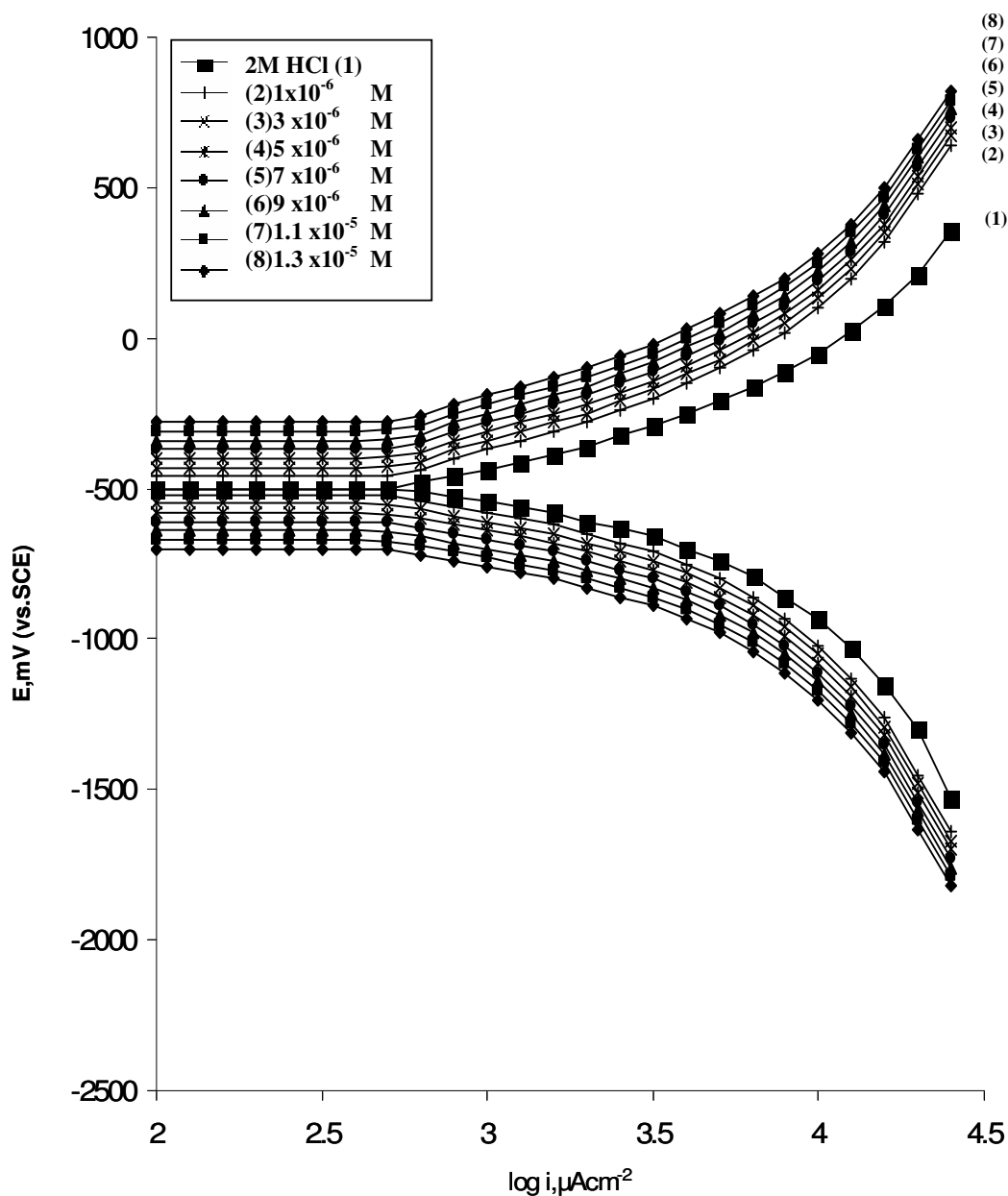


Figure 5. Galvanostatic polarization curves for α -brass in 2M HCl in absence and presence of different concentrations of inhibitor (c) at 303K

Table 5. Electrochemical parameters obtained from galvanostatic polarization of α -brass in 2M HCl containing different concentrations of inhibitors

Compound	[Inhibitor]. M	$-E_{\text{corr.}}$ (mV)SCE	$I_{\text{corr.}}$ (mAcm ⁻²)	β_a (mVdec ⁻¹)	β_c (mVdec ⁻¹)	θ	%IE
A	2M HCl	480	4425	1211	-1209	0	0
	1x10 ⁻⁶	492	2405	946	-1169	0.4565	45.65
	3x10 ⁻⁶	499	2210	971	-1160	0.5006	50.06
	5x10 ⁻⁶	506	1992	973	-1118	0.5499	54.99
	7x10 ⁻⁶	509	1824	898	-1104	0.5878	58.78
	9x10 ⁻⁶	515	1621	823	-937	0.6336	63.36
	11x10 ⁻⁶	521	1449	814	-923	0.6726	67.26
	13x10 ⁻⁶	527	1305	829	-922	0.7051	70.51
B	2M HCl	480	4425	1211	-1209	0	0
	1x10 ⁻⁶	498	2117	898	-778	0.5215	52.15
	3x10 ⁻⁶	505	1878	908	-765	0.5754	57.55
	5x10 ⁻⁶	509	1727	887	-768	0.6096	60.96
	7x10 ⁻⁶	513	1479	849	-972	0.6657	66.57
	9x10 ⁻⁶	516	1287	834	-895	0.709	70.9
	11x10 ⁻⁶	519	1147	811	-834	0.7408	74.08
	13x10 ⁻⁶	523	970	782	-808	0.7807	78.07
C	2M HCl	480	4425	1211	-1209	0	0.00
	1x10 ⁻⁶	492	1811	838	-678	0.5907	59.08
	3x10 ⁻⁶	493	1397	740	-611	0.6841	68.42
	5x10 ⁻⁶	500	1202	745	-587	0.7282	72.83
	7x10 ⁻⁶	505	1000	691	-550	0.7740	77.41
	9x10 ⁻⁶	512	859	699	-552	0.8058	80.59
	11x10 ⁻⁶	516	738	676.	-546	0.8331	83.32
	13x10 ⁻⁶	525	630	682	-539	0.8574	85.74
D	2M HCl	480	4425	1211	-1209	0	0
	1x10 ⁻⁶	502	3415	1247	-1356	0.2284	22.84
	3x10 ⁻⁶	509	3131	1209	-1178	0.2924	29.24
	5x10 ⁻⁶	512	2614	1072	-1033	0.4093	40.93
	7x10 ⁻⁶	514	2336	1076	-999	0.4722	47.22
	9x10 ⁻⁶	516	1815	1099	-953	0.5898	58.98
	11x10 ⁻⁶	524	1671	1042	-890	0.6222	62.22
	13x10 ⁻⁶	529	1461	1019	-776	0.6698	66.98

3.6. Pitting corrosion

Fig 6. shows the potentiodynamic anodic polarization curves of α -brass in solutions of 2M HCl + 0.05 M NaCl (as a pitting corrosion agent) devoid of and containing different concentrations of compound C as an example of the tested compounds at a scanning rate 1 mV/s. Similar curves were obtained for other compounds (not shown). The potential was swept from negative potential towards anodic direction up to the pitting potential. No any anodic oxidation peaks are observed in all anodic scan. The pitting potential (E_{pitt}) was taken as the potential at which the current owing, along the passive film increases suddenly to higher values, denoting the destruction of passive film and initiation

of visible pits. It was found that increasing the concentrations of these compounds cause a shift of the pitting potential in the noble direction indicating an increased resistance to pitting attack

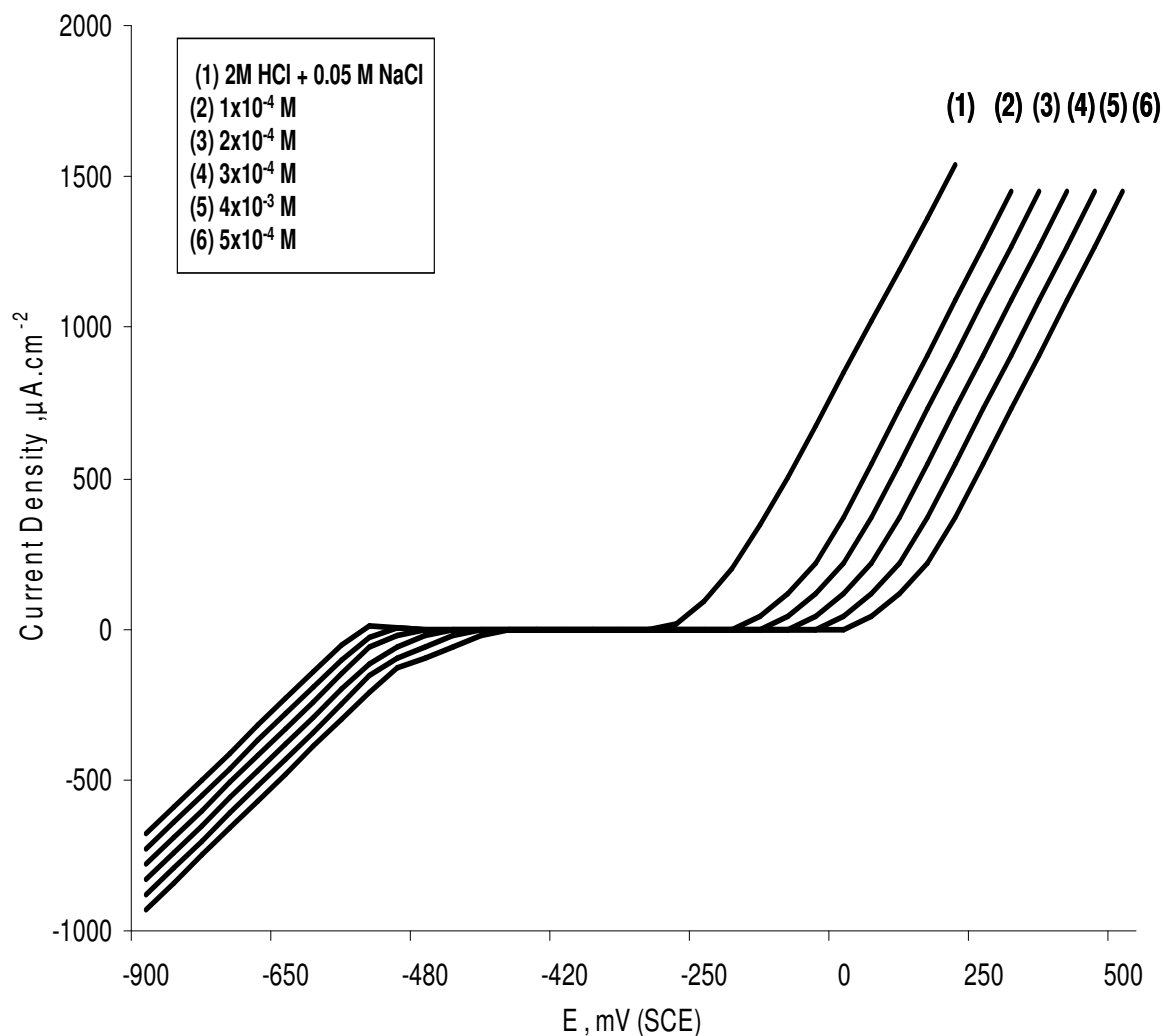


Figure 6. Potentiodynamic anodic polarization curves of α - brass in 2M HCl and 0.05 M NaCl containing different concentration of inhibitor (C)
 1) 0.00M 2) 1×10^{-4} M 3) 2×10^{-4} M
 4) 3×10^{-4} M 5) 5×10^{-3} M 6) 5×10^{-4} M compound (D)

The effect of addition of increasing concentrations of a phenylhydrazone derivatives on the values of pitting potential is illustrated in Fig. 7. This figure represents the relationship between E_{pitt} and logarithmic of molar concentration of additives. It is clear from this figure that, as the concentration of additives increases, the pitting potential shifted to more positive values in accordance with the following equation (7):

$$E_{pitt} = a + b \log C_{inh} \tag{7}$$

where a and b are constants depending on the type of additives used and the nature of the electrode. The positive shift of E_{pitt} indicates the increase resistance to pitting attack. At one and the same inhibitor concentration the marked shift of potential in the positive direction (increased resistant to pitting corrosion) decreases in the following sequence:

$$\text{compound C} > \text{compound B} > \text{compound A} > \text{compound D}$$

The different techniques used in this study gave the same order of inhibition efficiency but yielded different absolute values, probably due to the different experimental conditions.

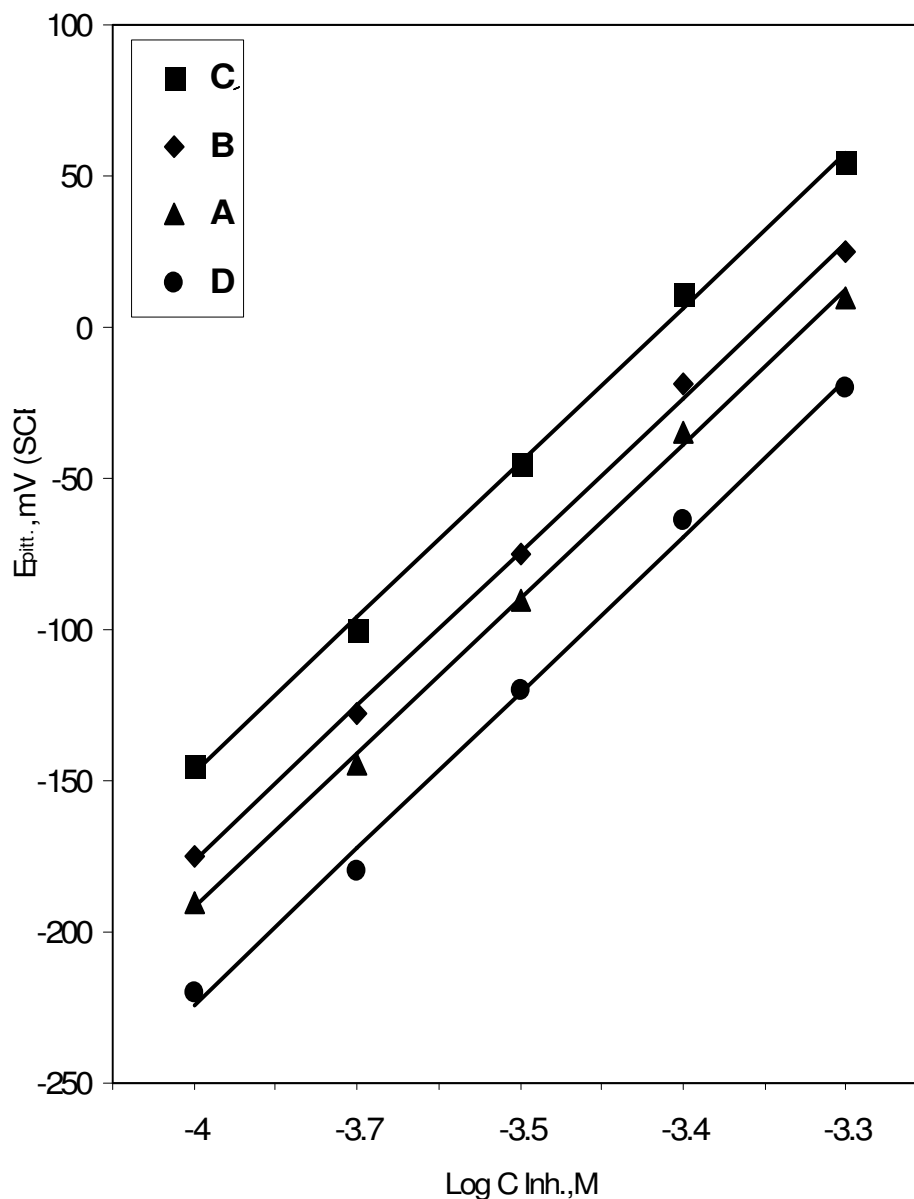
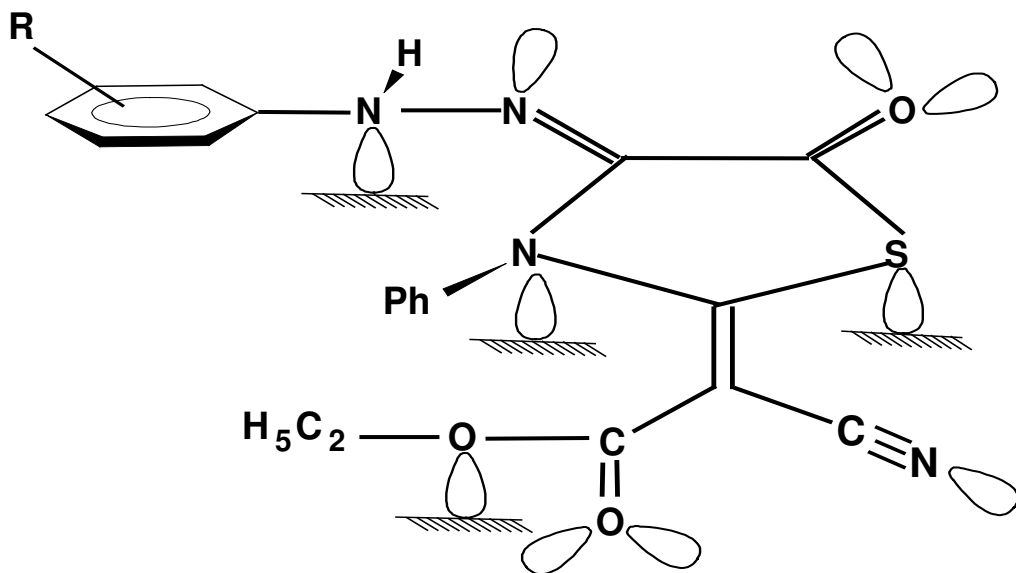
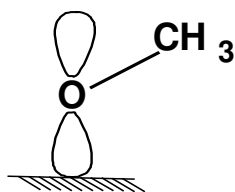


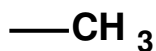
Figure 7. The relationship between pitting potential of α -brass and logarithm the different concentrations of the second group inhibitors in 2M HCl + 0.05M NaCl



R = para or meta



R = para or meta



R = para or meta

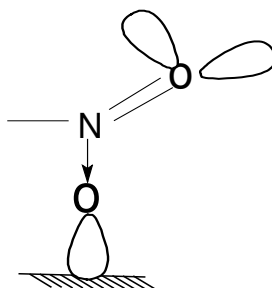


Figure 8. Skeletal representation of the mode of adsorption of phenylhydrazone derivatives

3.7. Chemical structure and corrosion inhibition

Inhibition of the α -brass corrosion in 2M HCl solution by phenylhydrazone derivatives using the above techniques was found to depend on the number of adsorption sites in the molecule and their charge density, molecular size and stability of these derivatives in acidic solutions. The inhibition effect of these compounds is attributed to the adsorption of the inhibitor molecules on the metal surface. The adsorption is assumed to take place mainly through the sulfur, nitrogen, oxygen atoms attached to the hetero ring and nitrogen in (N-NH) group (active centers). Transfer of lone pairs of electrons on the sulfur, nitrogen, oxygen to the surface to form coordinate type linkage is favored by the presence of vacant orbital in copper and zinc atoms of low energy. Polar character of constituent in the changing part of the inhibitor molecule seems to have a prominent effect on the electron charge density of the molecule. Skeletal representation of the mode of adsorption of the aminopyrimidine compounds is shown in Fig. 8 and clearly indicates the adsorption centers.

From the above sequence of IE, it is clear that the Compound (C) is the most efficient inhibitor because of the presence of highly electron releasing p-OCH₃ ($\sigma = -0.27$) which enhances the delocalized π -electrons on the active centers of the compound, in addition to it has six centers of adsorption (three nitrogen atoms, oxygen, sulphur, oxygen and one oxygen of -OCH₃ group). Compound (B) ($\sigma = -0.17$) comes after compound (C) in inhibition efficiency. This due to, it has only five active adsorption centers (three nitrogen atoms, oxygen, sulphur, oxygen) and p-CH₃ is lower in electron density than p-OCH₃ group. Compound (A) ($\sigma = 0.0$) comes after compound (B) in percentage inhibition, this due to its lower molecular size than compounds (C) and (B) and lower sharing electron density to the molecule. Compound (F) comes after compound (A) in percentage inhibition. This is due to both p- NO₂ group are electron withdrawing groups with positive Hammett constants ($\sigma = + 0.78$) and their order of inhibition depends on the magnitude of their withdrawing character.

4. CONCLUSIONS

1. Phenylhydrazone derivatives act as an inhibitors for corrosion of α -brass in 2M HCl solution.
2. The inhibition efficiency increases with increase in the concentration of these inhibitors but decreases with an increase in temperature.
3. The addition of KI to these compounds improve the values of inhibition efficiency due to synergistic effect.
4. The inhibition is due to the adsorption of the inhibitor molecule on the brass surface.
5. The adsorption of these compounds on the brass surface follows Temkin adsorption isotherm.
6. Phenylhydrazone derivatives provide protection against pitting corrosion of α -brass in presence of chloride ions.

References

1. E. Stupnisek-Lisac, A. Loncaric Bozic and I. Cafuk, *Corros.* 54 (1998) 713.
2. R. Gasparac, C.R. Martin and E. Stupnisek-Lisac, *J. Electrochem. Soc.* 147 (2000) 548.
3. A.M. Zaky, *Br. Corros. J.* 36 (2001) 59.
4. R.F. North and M.J. Pryar, *Corros. Sci.* 10 (1970) 297.
5. M.A. Elmorsi, M.Y. EL-Sheikh, A.M. Bastweesy and M.M. Ghoneim, *Bull. Electrochem.* 7 (1991) 158.
6. M.M. Osman, *Mater. Chem. Phy.* 71 (2001) 12.
7. M.A. Quraishi, I.H. Farooqi and P.A. Saini, *Br. Corros. J.* 35 (2000) 78.
8. H.C. Shih and R.J. Tzou, *J. Electrochem. Soc.* 138 (1991) 958.
9. G. Quartarone, G. Moretti and T. Bellami, *Corros.* 54 (1998) 606.
10. A.G. Gad-Allah, M.M. Abou-Romia, M.W. Badawy and H.H. Rehan, *J. Appl. Electrochem.* 21 (1991) 829.
11. A.K. Mitra, *R&D J., NTPC* 2 (1996) 52.
12. M.A. Elmorsi and A.M. Hassanein, *Corros. Sci.* 41 (1999) 2337.
13. F. Ammeloot, C. Fiaud and E.M.M. Sutter, *Electrochim. Acta* 43 (1997) 3565.
14. A.G. Gad Allah, M.W. Badawy, H.H. Rehan and M.M. Abou-Romia, *J. Appl. Electrochem.* 19 (1989) 982.
15. G. Trabanelli, G. Brunoro, C. Monticelli and M. Foganolo, *Corros. Sci.* 25 (1985) 1019.
16. L.F.A. Sylvia da Costa, M.L. Agostinho and K. Nobe, *J. Electrochem. Soc.* 140 (1993) 3483.
17. P. Gupta, R.S. Chaudhury, T.K.G. Namboodhary and B. Prakash, *Corros. Sci.* 33 (1983) 1361
18. P. Gupta, R.S. Chaudhury, T.K.G. Namboodhary and B. Prakash, *Br. Corros. J.* 17 (1982) 136.
19. S. Kertit, H. Es-Soufi, B. Hammouti, M. Benkaddour, *J. Chem. Phys.* 95 (1998) 207.
20. M.M. Singh, R.B. Rastogi and B.N. Upadhyay, *Corros.* 50 (1994) 620.
21. J.A. Schreifels, T. Bagwell and J.J. Weers, *Corros.* 45 (1989) 84.
22. O. Hollander and R.C. May, *Corros.* 41 (1985) 39.
23. M. Oertel, P. Klusener, M. Kempken, A. Benninghoven, H.J. Rother and R. Holm, *Appl. Surf. Sci.* 37 (1989) 135.
24. G.D. Zhou, S.M. Cai, L.Q. Song, H.Q. Yang, A. Fujishima, A. Ibrahim, Y.G. Lee and B.H. Loo, *Appl. Surf. Sci.* 529 (1991) 227.
25. P.F. Lynch, C.W. Brown and R. Heidersbach, *Corros.* 39 (1983) 357.
26. D.W. Deberry, G.R. Peyton and W.S. Clark, *Corros.* 40 (1984) 250.
27. H.A.A. El-Rahman, *Corros.* 47 (1991) 424.
28. S.L.F.A. da Costa, S.M.L. Agostinho, H.C. Chagas and J.C. Rubim, *Corros.* 43 (1987) 149.
29. P.B. Mathur and T. Vasudevan, *Corros.* 38 (1982) 17.
30. S.M. Abd El-Haleem, A.A. Abdel Fattah and W. Taylor, *Res. Mech.* 30 (3) (1985) 333.
31. K. Aramaki and N. Hackerman, *J. Electrochem. Soc.* 116 (1969) 568.
32. I. Putilova, S. Balezin, I.N. Barannik and V.P. Bishop, *Metall. Corros. Inhibit.*, Pergamon, Oxford, (1960), 196p.
33. S.S. Abd El-Rehim, S.A.M. Refaey, F. Taha, M.B. Saleh and R.A. Ahmed, *J. Appl. Electrochem.* 31 (2001) 429.